

ANALYZING SINGLE BARRETTES AS RIGID SUPPORT BY COMPOSED COEFFICIENT TECHNIQUE

Mahmoud El Gendy^{1*}, Hassan Ibrahim¹ & Ibrahim El Arabi¹

Department of Civil Engineering, Faculty of Engineering, Port Said University, Egypt, 42526
Port Said, Egypt

*Corresponding Author: Mahmoud_gendy1@hotmail.com

Abstract: Most of soil structure interaction methods for analyzing large-section supports such as barrette foundation modeling the barrette and surrounding soil using 3D FE model. In which, the model leads to a large finite element mesh of a large system of linear equations to be solved. In this paper, a Composed Coefficient Technique (CCT) is adapted for analyzing barrette. The technique takes into account the 3D full interactions between barrette and the surrounding soil. Due to the high rigidity of the barrette relative to the surrounding soil, a uniform settlement along the barrette height can be considered. This enables to compose the stiffness coefficients of the soil matrix into composed coefficients, which consequently leads to a significant reduction in the soil stiffness matrix. The validity and the examinations presented in this research work were carried out with an application for analyzing barrette by CCT. This analysis can be extended for modeling the nonlinear behavior of single barrette and barrette-raft. In which, the barrette can be treated as single unit having a uniform settlement.

Keywords: *Soil structure interaction, deep foundation, barrette, settlement.*

1.0 Introduction

Heavy loaded structures need to be supported on deep foundations such as barrette. Analyzing this system of foundation is a complex task because it is a three-dimensional problem including the interaction between barrettes and soil. Considering this interaction requires a long computational time where a huge soil matrix is required to verify the compatibility among barrette and soil. The standard models for analyzing this complex problem depend on a full three-dimensional analysis, which leads to very large number of elements, and thus these models are time consuming even for the fast computers of today, especially when analyzing barrette group or barrette raft. A similar foundation element of pile maybe considered as a less complicated problem than that of the barrette cross section. Piles in most cases are circular in shape with small cross-section area, while that of the barrette is large with a rectangular shape. Therefore, pile can be treated as a beam member exposed to point loads on its nodes, while barrette

treated as a block member. There are many available methods used to analyze piles most of them are used also to analyze barrette with equivalent cross section area to that of the pile (Basu *et al.*, 2008; Lei *et al.*, 2007 ; Seo *et al.*, 2009).

Other alternative methods to analyze the barrettes are those using the full three dimensional finite element methods (Fellenius *et al.*, 1999; Thasnanipan *et al.*, 1998; Thasnanipan *et al.*, 2001; Shulyatiev *et al.*, 2013; Lin *et al.*, 2014). For single pile, pile group and piled raft, El Gendy (2007) presented a technique based on the flexibility coefficients an efficient analysis by using Composed Coefficient Technique (CCT) to reduce the size of the entire soil stiffness matrix. In this technique, the pile is treated as a rigid member having a uniform settlement for all nodes along its shaft and base. CCT enables to assemble pile coefficients in composed coefficients. This technique is applied efficiently for many studies (Hattab, 2007; Reda, 2009; Rabiei, 2009, 2010, 2016; Kamash, 2009, 2012; Kamash *et al.*, 2014; Ibrahim *et al.*, 2009; Mobarak, 2010; El-Labban, 2011; Moubarak, 2013; Chieruzzi *et al.*, 2013; El Gendy *et al.*, 2013, 2014). This technique is also further developed to be used in this study for analyzing the barrette based on both flexibility coefficients and full 3D FE. The Advantage of the CCT is that interaction of soil elements with the barrette elements are taken into consideration. The proposed analysis reduces considerably the number of equations that needs to be solved. Another point of view to choice of the CCT for the barrette analysis is that the designer is interested in the soil settlements and contact forces at different levels on the barrette height not at each barrette node. The application of CCT enables the nonlinear response of the barrette by a hyperbolic relation between the load and settlement of the barrette.

2.0 Mathematical Modeling

2.1 Modeling Single Barrette Using Flexibility Coefficients

Following the CCT for modeling pile foundation by El Gendy (2007), a composed coefficient k_s [kN/m] representing the soil stiffness of the barrette is developed. The mathematical formulation of the composed coefficient k_s for different cases of barrette analyses will be described in the forthcoming items.

2.1.1 Soil Stiffness Matrix

The rectangular cross sectional barrette shown in Figure 1 is divided into a number of shaft elements and base elements with n_s nodes, each acted upon by a distributed stress. To carry out the analysis, the stresses acting on shaft and base elements are replaced by a series of concentrated forces acting on nodes.

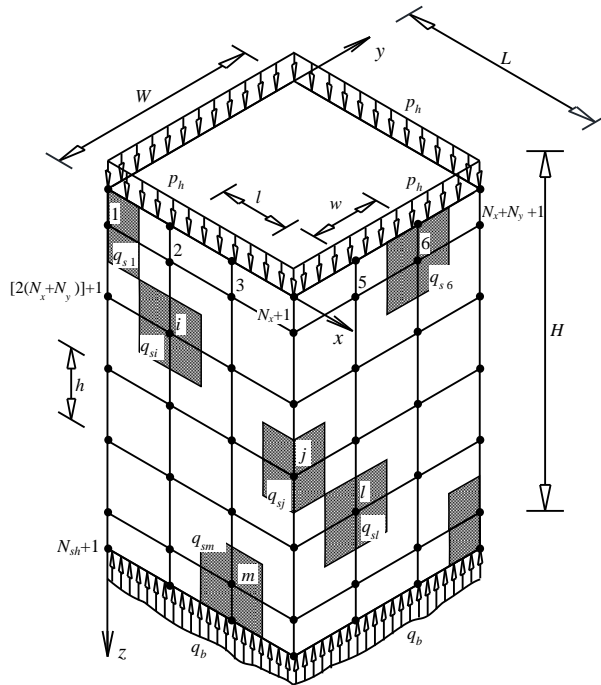


Figure 1: Barrette geometry, elements and stresses

The settlement of the soil at any node i of the barrette may be rewritten in general form as:

$$s_i = \sum_{j=1}^{n_s} I_{i,j} Q_j \tag{1}$$

where: s_i is soil settlement on any node i either on the shaft or on the base, (m); Q_j is contact force on node j , (kN); Q_j represents either the forces on shaft nodes or base nodes; n_s is total number of contact nodes; $I_{i,j}$ is flexibility coefficient of node i due to a unit force on node j (m/kN). Closed form equations for these coefficients are described in the Appendix A. Eq. 1 for settlements of the soil adjacent to all nodes of the barrette may be written in a matrix form as:

$$\{s\} = [Is] \{Q\} \tag{2}$$

where $\{s\}$ is n_s settlement vector; $\{Q\}$ is n_s contact force vector; $[Is]$ is $n_s \times n_s$ soil flexibility matrix. Inverting the soil flexibility matrix in Eq. 2, leads to:

$$\{Q\} = [ks] \{s\} \tag{3}$$

where $[ks]$ is $n_s \times n_s$ soil stiffness matrix, $[ks] = [Is]^{-1}$.

2.1.2 Rigid Analysis

The barrette is a huge concrete volume, which may be considered as a rigid body subjected to vertical loads and moves vertically with a uniform displacement, $w_0 = s_1 = s_2 = \dots = s_{n_s}$ on all its nodes. Therefore, the unknowns of the problem are reduced to n_s contact forces and the rigid body displacement w_0 . Carrying out the summation of all contact forces in the Eq. 3, leads to:

$$\sum_{i=1}^{n_s} Q_i = w_0 \sum_{i=1}^{n_s} \sum_{j=1}^{n_s} k_{i,j} \quad (4)$$

where $k_{i,j}$ are the coefficients of the soil stiffness matrix $[ks]$. Eq.4 may be rewritten as:

$$Ph = ks w_0 \quad (5)$$

where the applied force Ph (kN) on the barrette head is the sum of all contact forces Q_i ,

$Ph = \sum_{i=1}^{n_s} Q_i$, while the composed coefficient ks (kN/m) is the sum of all coefficients of the soil stiffness matrix, $ks = \sum_{i=1}^{n_s} \sum_{j=1}^{n_s} k_{i,j}$.

Eq.5 gives the linear relation between the applied load on the barrette head and the uniform settlement w_0 of all barrette nodes. For a single barrette, the applied load on the barrette head Ph is given and hence the uniform settlement w_0 can be determined from Eq. 5. Substituting the value of w_0 in Eq. 3, gives n_s unknown contact forces Q_i in case of considering the barrette as full rigid body.

2.2 Modeling Barrette and Subsoil Using 3D Finite Elements

The barrette and the surrounding subsoil are represented by 3D finite elements as shown in Figure 2, which presented a quarter of the mesh and barrettes. Then, the finite element method is used for analyzing the barrette and subsoil medium together using solid block elements. Each element consists of eight nodes; each node has forces and displacements in the three directions. The composed coefficient technique is used to perform the analysis of the single barrette and barrette group.

The next paragraphs illustrate the generation of a stiffness matrix of composed coefficients for a single barrette. The same procedure can be applied for barrette groups or barrette raft. Consider the simple finite element mesh in the cross section of a barrette and subsoil shown in Figure 3 as an example. The subsoil has the nodes from 1 to 69, while the barrette has the nodes 70 to 90.

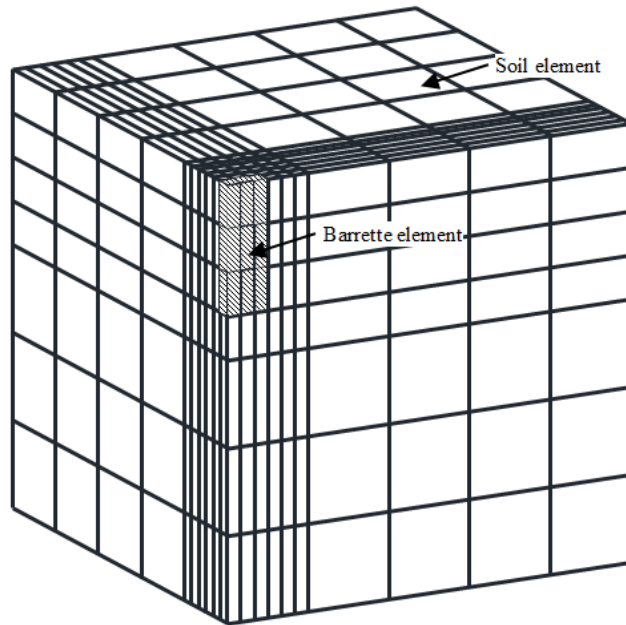


Figure 2: Quarter mesh of 3D finite elements of a barrette and the surrounding subsoil

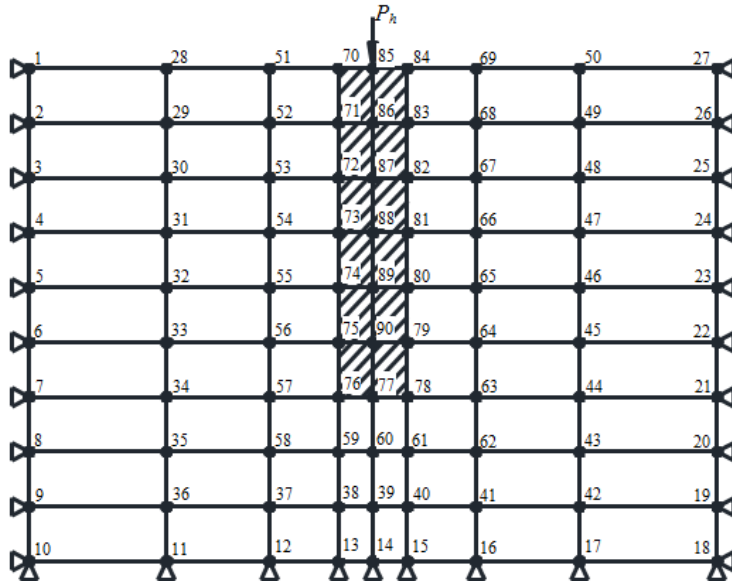


Figure 3: Simple finite element mesh in a cross section of the barrette and subsoil

The global stiffness matrix equation of the system of the single barrette and the surrounding subsoil can be expressed as:

$$\{P\} = [kp]\{\delta\} \quad (6)$$

where $\{\delta\}$ is $3n$ displacement vector $\{u, v, w\}$; $\{P\}$ is $3n$ vector of applied load $\{p_x, p_y, p_z\}$; $[kp]$ is $(3n \times 3n)$ Stiffness matrix; n is number of the total nodes.

The barrette nodes in the matrix equation, Eq. (6) are rearranged to be at the end of the matrix. Considering uniform displacements in the three directions due to the high barrette rigidity and carrying out the summation of the corresponding stiffness coefficients, Eq. (6) can be rewritten and expanded as:

$$\begin{pmatrix} P_{x1} \\ P_{y1} \\ P_{z1} \\ \dots \\ P_{x69} \\ P_{y69} \\ P_{z69} \\ \dots \\ P_{x70} \\ P_{y70} \\ P_{z70} \\ \dots \\ P_{x90} \\ P_{y90} \\ P_{z90} \end{pmatrix} = \begin{bmatrix} k_{1,1} & k_{1,2} & k_{1,3} & \dots & k_{1,205} & \dots & \dots & \dots & k_{1,210} & \dots & k_{1,268} & k_{1,269} & k_{1,270} \\ k_{2,1} & k_{2,2} & k_{2,3} & \dots & k_{2,205} & \dots & \dots & \dots & k_{2,210} & \dots & k_{2,268} & k_{2,269} & k_{2,270} \\ k_{3,1} & k_{3,2} & k_{3,3} & \dots & k_{3,205} & \dots & \dots & \dots & k_{3,210} & \dots & k_{3,268} & k_{3,269} & k_{3,270} \\ \dots & \dots \\ k_{205,1} & k_{205,2} & k_{205,3} & \dots & k_{205,205} & \dots & \dots & \dots & k_{205,210} & \dots & k_{205,268} & k_{205,269} & k_{205,270} \\ k_{206,1} & k_{206,2} & k_{206,3} & \dots & k_{206,205} & \dots & \dots & \dots & k_{206,210} & \dots & k_{206,268} & k_{206,269} & k_{206,270} \\ k_{207,1} & k_{207,2} & k_{207,3} & \dots & k_{207,205} & \dots & \dots & \dots & k_{207,210} & \dots & k_{207,268} & k_{207,269} & k_{207,270} \\ k_{208,1} & k_{208,2} & k_{208,3} & \dots & k_{208,205} & \dots & \dots & \dots & k_{208,210} & \dots & k_{208,268} & k_{208,269} & k_{208,270} \\ k_{209,1} & k_{209,2} & k_{209,3} & \dots & k_{209,205} & \dots & \dots & \dots & k_{209,210} & \dots & k_{209,268} & k_{209,269} & k_{209,270} \\ k_{210,1} & k_{210,2} & k_{210,3} & \dots & k_{210,205} & \dots & \dots & \dots & k_{210,210} & \dots & k_{210,268} & k_{210,269} & k_{210,270} \\ \dots & \dots \\ k_{268,1} & k_{268,2} & k_{268,3} & \dots & k_{268,205} & \dots & \dots & \dots & k_{268,210} & \dots & k_{268,268} & k_{268,269} & k_{268,270} \\ k_{269,1} & k_{269,2} & k_{269,3} & \dots & k_{269,205} & \dots & \dots & \dots & k_{269,210} & \dots & k_{269,268} & k_{269,269} & k_{269,270} \\ k_{270,1} & k_{270,2} & k_{270,3} & \dots & k_{270,205} & \dots & \dots & \dots & k_{270,210} & \dots & k_{270,268} & k_{270,269} & k_{270,270} \end{bmatrix} \begin{pmatrix} u_1 \\ v_1 \\ w_1 \\ \dots \\ u_{69} \\ v_{69} \\ w_{69} \\ \dots \\ u_{70} \\ v_{70} \\ w_{70} \\ \dots \\ u_{90} \\ v_{90} \\ w_{90} \end{pmatrix} \quad (7)$$

where $k_{i,j}$ is the stiffness coefficient of the global stiffness matrix.

Equating displacements in each direction of all nodes on the barrette by uniform displacements u_x , v_y and w_z and carrying out the summation of rows and columns related to that displacements in Eq. (7), gives the composed coefficients with the force on the barrette Q_x , Q_y and Q_z as follows:

$$\begin{pmatrix} P_{x1} \\ P_{y1} \\ P_{z1} \\ \dots \\ P_{x69} \\ P_{y69} \\ P_{z69} \\ Q_x \\ Q_y \\ Q_z \end{pmatrix} = \begin{pmatrix} k_{1,1} & k_{1,2} & \dots & \dots & \dots & k_{1,206} & k_{1,207} & \sum_{j=70}^{90} k_{1,\beta} & \sum_{j=70}^{90} k_{1,j2} & \sum_{j=70}^{90} k_{1,j\beta} \\ k_{2,1} & k_{2,2} & \dots & \dots & \dots & k_{2,206} & k_{2,207} & \sum_{j=70}^{90} k_{2,\beta} & \sum_{j=70}^{90} k_{2,j2} & \sum_{j=70}^{90} k_{2,j\beta} \\ k_{3,1} & k_{3,2} & \dots & \dots & \dots & k_{3,206} & k_{3,207} & \sum_{j=70}^{90} k_{3,\beta} & \sum_{j=70}^{90} k_{3,j2} & \sum_{j=70}^{90} k_{3,j\beta} \\ \dots & \dots \\ k_{205,1} & k_{205,2} & \dots & \dots & \dots & k_{205,206} & k_{205,207} & \sum_{j=70}^{90} k_{205,\beta} & \sum_{j=70}^{90} k_{205,j2} & \sum_{j=70}^{90} k_{205,j\beta} \\ k_{206,1} & k_{206,2} & \dots & \dots & \dots & k_{206,206} & k_{206,207} & \sum_{j=70}^{90} k_{206,\beta} & \sum_{j=70}^{90} k_{206,j2} & \sum_{j=70}^{90} k_{206,j\beta} \\ k_{207,1} & k_{207,2} & \dots & \dots & \dots & k_{207,206} & k_{207,207} & \sum_{j=70}^{90} k_{207,\beta} & \sum_{j=70}^{90} k_{207,j2} & \sum_{j=70}^{90} k_{207,j\beta} \\ \sum_{i=70}^{90} k_{i1,1} & \sum_{i=70}^{90} k_{i1,2} & \dots & \dots & \dots & \sum_{i=70}^{90} k_{i1,206} & \sum_{i=70}^{90} k_{i1,207} & \sum_{i=70}^{90} \sum_{j=70}^{90} k_{i1,\beta} & \sum_{i=70}^{90} \sum_{j=70}^{90} k_{i1,j2} & \sum_{i=70}^{90} \sum_{j=70}^{90} k_{i1,j\beta} \\ \sum_{i=70}^{90} k_{i2,1} & \sum_{i=70}^{90} k_{i2,2} & \dots & \dots & \dots & \sum_{i=70}^{90} k_{i2,206} & \sum_{i=70}^{90} k_{i2,207} & \sum_{i=70}^{90} \sum_{j=70}^{90} k_{i2,\beta} & \sum_{i=70}^{90} \sum_{j=70}^{90} k_{i2,j2} & \sum_{i=70}^{90} \sum_{j=70}^{90} k_{i2,j\beta} \\ \sum_{i=70}^{90} k_{i3,1} & \sum_{i=70}^{90} k_{i3,2} & \dots & \dots & \dots & \sum_{i=70}^{90} k_{i3,206} & \sum_{i=70}^{90} k_{i3,207} & \sum_{i=70}^{90} \sum_{j=70}^{90} k_{i3,\beta} & \sum_{i=70}^{90} \sum_{j=70}^{90} k_{i3,j2} & \sum_{i=70}^{90} \sum_{j=70}^{90} k_{i3,j\beta} \end{pmatrix} \begin{pmatrix} u_1 \\ v_1 \\ w_1 \\ \dots \\ u_{69} \\ v_{69} \\ w_{69} \\ u_x \\ v_y \\ w_z \end{pmatrix} \quad (8)$$

where Q_x is sum of horizontal forces in x-direction on all barrette nodes, $Q_x = \sum P_x = 0$; Q_y is sum of horizontal forces in y-direction on all barrette nodes, $Q_y = \sum P_y = 0$; Q_z is sum of vertical forces on all barrette nodes, $Q_z = \sum P_z = Ph$; u_x is uniform displacement in x-direction on all barrette nodes, $u_x = u_{70} = \dots = u_{90}$. v_y is uniform displacement in y-direction on all barrette nodes, $v_x = v_{70} = \dots = v_{90}$; w_z is uniform displacement in z-direction on all barrette nodes, $w_x = w_{70} = \dots = w_{90}$; $i1=3i-2$, $i2=3i-1$, $i3=3i$, $j1=3j-2$, $j2=3j-1$, $j3=3j$. Solving the above system of linear equations, gives the displacement at each node, in which the vertical displacement is equal to the soil settlement at that node. Substituting barrette displacements from Eq. (8) in Eq. (7), gives contact forces on the barrette.

3.0 Numerical Results

The proposed method for analyzing barrette using *CCT* outlined in this paper was implemented in the program *ELPLA*. With the help of this program, an analysis of two verification examples is carried out first to judge the proposed method for both linear and nonlinear analyses. Then, a comparative examination of modeling for analyzing single barrette is carried out. Finally, case studies for barrettes on the soil of the new area of East Port Said are presented.

3.1 Validity of Nonlinear Analysis of Single Barrette

Thasnsnipan *et al.* (1998) and Lin *et al.* (2014) carried out load tests of single barrettes having a rectangular cross section embedded in a multi-layered soil medium. In the load tests, results of barrette load tests are obtained from Bangkok, Thailand subsoil area and Taipei, Thailand subsoil area.

The load on the barrette head and barrette geometry for the chosen cases are listed in Table 1 and Table 2. The subsoil of each case consists of different layers, each layer having a different Modulus of Elasticity E_s and *Poisson's* ratio ν_s , as listed in Table 3 and Table 4 (Thasnsnipan *et al.*, 1998; Plaxis Bulletin, 2012).

Table 1: Loads and barrette geometries

Load (kN)	Height (m)	Cross section
14000		
28000	61.8	0.82 m × 2.7 m
35000		

Table 2: Barrette geometries

Height (m)	Cross section
44	0.80 m × 2.5 m

Table 3: Subsoil properties

Layer No.	z (m)	E_s (kN/m ²)	ν_s (-)
1	12.5	5000	0.33
2	23	60000	0.33
3	37	80000	0.3
4	40	20000	0.33
5	53	80000	0.30
6	58	20000	0.33
7	∞	80000	0.30

Table 4: Subsoil properties

Layer No.	z (m)	E_s (kN/m ²)	ν_s (-)
1	26.46	93793	0.25
2	28.40	253293	0.25
3	30.44	221593	0.25
4	33.60	88391	0.25
5	36.80	131381	0.25
6	40.80	192106	0.25
7	42.44	166948	0.25
8	∞	229738	0.25

A comparison of the results of a single barrettes in a multi-layered soil medium of the present analysis using flexibility coefficient with Thasnsnipan *et al.* (1998) and Lin *et al.* (2014) are presented herein, The height of the barrette is divided into equal elements, each element has a height of $h = 1.0$ (m). Both the barrette length and width are divided into four equal elements. The barrettes are analyzed nonlinearly using a hyperbolic function to represent the real load settlement curve relation. In the analysis, the barrette is assumed to be fully rigid having a uniform settlement.

A limit barrette load Ql has been used as a parameter geometry for the hyperbolic curve of nonlinear response of load settlement relation. (Russo, 1998) suggested a limiting shaft friction not less than 180 kN/m² meeting undrained shear strength of 200 kN/m². To carry out the present nonlinear analysis a limit shaft friction of $ql = 220$ kN/m² is considered, which gives a limit barrette load of $Ql = 96$ MN to compare with the result with those of (Thasnsnipan *et al.*, 1998), A limit barrette load of $Ql = 50$ MN is taken, to compare with the result with those of (Lin *et al.*, 2014), where it is assumed from the load settlement curve of (Lin *et al.*, 2014).

The barrette load-settlement relations obtained from the present nonlinear analysis using flexibility coefficient are compared with those of the load tests carried out by

(Thasnsnipan *et al.*, 1998; Lin *et al.*, 2014) in Figure 4 and Figure 5 respectively. From these figures, it can be concluded that the difference of the measured and computed settlement is less than 10.0 [%], which have a very small value of 0.04 cm and 0.16 cm compared with those of (Thasnsnipan *et al.*, 1998; Lin *et al.*, 2014) respectively. It is also very small when compared to the barrette dimensions. It also shows that the verification of the load-settlement behavior of the present nonlinear analysis are in good agreement with those of measured load settlement tests carried out by (Thasnsnipan *et al.*, 1998; Lin *et al.*, 2014).

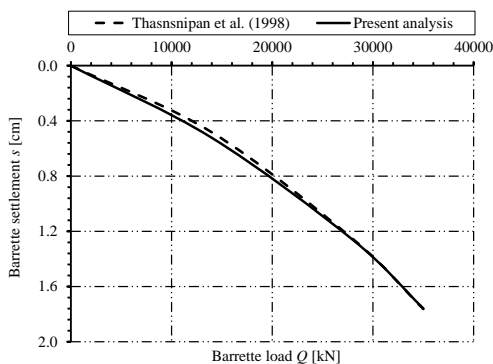


Figure 4: Load settlement curve

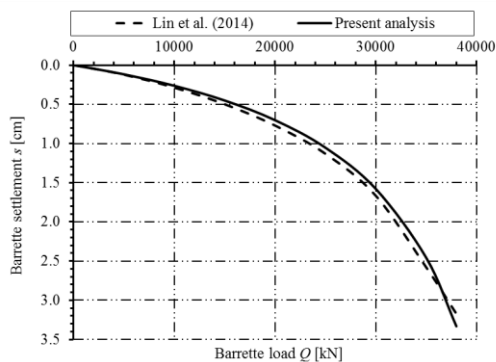


Figure 5: Load settlement curve

3.2 Examination of Models Used CCT with Those Used in Traditional 3D FE.

A single barrette having a rectangular cross section embedded in subsoil layers is analyzed using different numerical models, as follows:

- 1- Model (1): 3D finite element model of soil and CCT for barrette.
- 2- Model (2): Flexibility coefficient model of soil and CCT for barrette.
- 3- Model (3): 3D traditional finite element model analyzed by program SAP 3D.
- 4- Model (4): 3D traditional finite element model analyzed by program PLAXIS 3D.

In 3D traditional finite element models of SAP 3D and PLAXIS 3D the barrette-soil systems are represented by block elements. The composed coefficient technique CCT is implemented in both models presented in this study. In this case, the barrette is treated as a rigid body having uniform settlement. This technique reduces the commotional time and size of the problem as these two terms considered as main difficulties in the three dimensional problems.

The results of the four models are compared for verification. The barrette shown in Figure 6 is considered and analyzed linearly. Different loads on the barrette head with different dimensions are studied and not included in this paper. Only the barrette of 3.0

m length, 1.0 m width and 20.0 m height with a load of 2100 kN is presented in this paper as an example.

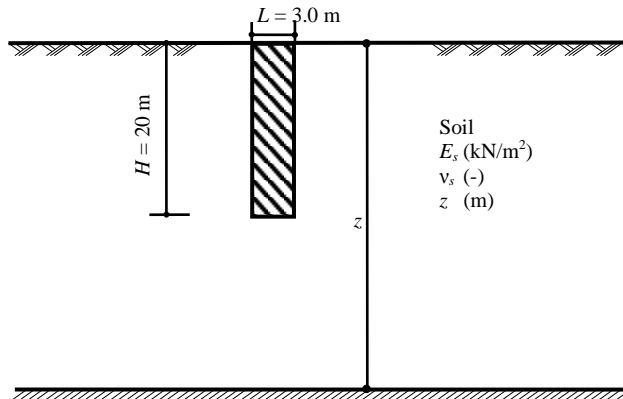


Figure 6: Single barrette with subsoil

Table 5: Subsoil properties

Soil	z [m]	E_s [kN/m ²]	v_s [-]
(A)	40	20000	0.30
(B)	40	5000	0.30
(C)	100	5000	0.30
(D)	40	20000	0.30
	100	5000	0.30
(E)	40	5000	0.30
	100	20000	0.30

As listed in Table 5, five study cases were considered, as follows:

- Case (A), (B) and (C) contains single soil layer.
- Case (D) includes two different soil layers with a relatively harder top layer.
- Case (E) includes two different soil layers with a relatively harder bottom layer.

For models 1 to 3, the height of the barrette is divided into equal elements, each of 2.0 m height. The barrette length and width are divided into two equal elements. In model 4 analyzed by PLAXIS 3D, the generation of the elements are created automatically and it chosen to be very fine. To ensure full interaction between the isotropic elastic half-space soil medium and the barrette, the dimension of the soil around the barrette is extended enough. To verify that many trial with different distances in the 3 spaces are carried out. The barrette is analyzed linearly and the barrette is assumed to be fully rigid having a uniform settlement.

In the first model, the barrette and the soil elements are solved as double symmetric system to reduce the number of equations to one quarter. Consequently, the computational time is also reduced. The barrette settlements obtained from the different models are compared. Table 6 shows the settlement results for the different models.

Table 6: Comparison between settlements obtained from different models

Case	Settlements [cm]			
	Present analysis		Model (3) SAP 3D	Model (4) PLAXIS 3D
	Model (1) 3D FE	Model (2) FC		
A	0.588	0.549	0.580	0.576
B	2.123	2.198	2.202	2.157
C	2.396	2.577	2.491	2.453
D	0.746	0.929	0.773	0.781
E	2.201	2.284	2.288	2.244

From those results, it can be seen that the results of the present study are in good agreement with those obtained by the other models for different cases.

3.3 Examination of Mathematical Models Using CCT

A single barrette having a rectangular cross section embedded in different subsoil conditions is analyzed using the two different models based on *CCT* technique:

1. 3D finite element model.
2. Flexibility coefficient model.

Results of 3D finite element model are compared with those using flexibility coefficient model. In 3D finite element model, the barrette-soil systems are represented by block elements, each consists of eight nodes. The composed coefficient technique *CCT* is implemented in both 3D finite element and flexibility coefficient models. In this case, the barrette is treated as a rigid body having uniform settlement. This technique reduces the commotional time and the size of the problem as these two terms considered as main difficulties in the three dimensional problems.

The purpose of the comparative study is showing the limitations and differences in both results and also to be a guideline to determine which model may be preferably used in the analysis. The barrette shown in Figure 7 is considered and analyzed linearly for twelve different cases of loads, subsoil and geometries. Analysis covered a wide range of variables of barrette length L and barrette height H . The effect of these variables on the settlement is also investigated. The barrette geometry for the chosen cases is listed in Table 7, while the loads on the barrette head of each case are listed in Table 8.

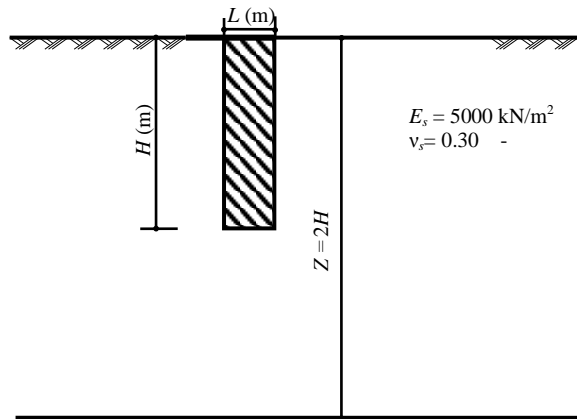


Figure 7: Single barrette with subsoil (A)

Table 7: Barrette geometries.

Length/ Height	$L = 1.5$	$L = 2.0$	$L = 2.5$	$L = 3.0$
$H = 20$	Case 1	Case 2	Case 3	Case 4
$H = 30$	Case 5	Case 6	Case 7	Case 8

Table 8: Barrette loads.

Length/ Height	$L = 1.5$	$L = 2.0$	$L = 2.5$	$L = 3.0$
$H = 20$	1050	1400	1750	2100
$H = 30$	1200	1600	2000	2400

Table 9: Subsoil properties.

Soil	z [m]	E_s [kN/m ²]	ν_s [-]
(A)	$2H$	5000	0.30
(B)	$0.4H$	5000	0.40
	$1.2H$	8000	0.35
	$2H$	10000	0.30
(C)	$0.6H$	5000	0.40
	$2H$	25000	0.30
(D)	$0.6H$	25000	0.30
	$2H$	5000	0.40

The eight cases of loads and geometries are analyzed with different subsoil as listed in Table 9 as follows:

- Soil (A) Single layer.
- Soil (B) Three different layers extended from a weak layer to a hard one.
- Soil (C) Two different layers, the first is a weak layer and the second is a hard one.
- Soil (D) Two different layers, the first is a hard layer and the second is a weak one.

A single barrette is analyzed in a single soil layer, and the height of the barrette is divided into equal elements, of 1.0 m height each. The barrette length and width are divided into two equal elements. To ensure full interaction between the isotropic elastic half-space soil medium and the barrette, the dimension of the soil around the barrette is extended enough. The barrette is analyzed linearly and the barrette is assumed fully rigid having a uniform settlement. In the 3D finite element model, the barrette and the soil elements are solved as double symmetric system to reduce the number of equations to quarter. Consequently, the computational time is also reduced. The barrette settlements obtained from both analyses are compared. Figure 8 to Figure 11 show the settlement results and the difference in the calculated settlements for the two models. From these figures and tables, it can be concluded that:

- For the four cases, settlements are identical for both models. The maximum difference in the settlement of both models lies between 0.1 cm and 0.2 cm, which is equal to a very small value when compared with the barrette dimensions.
- Finally, both flexibility coefficient and 3D finite element models can be used safely in the linear analysis of single barrette.
- Due to the less number of nodes in flexibility coefficient model rather than 3D finite element model, the first model consumes less computation time in the analysis.

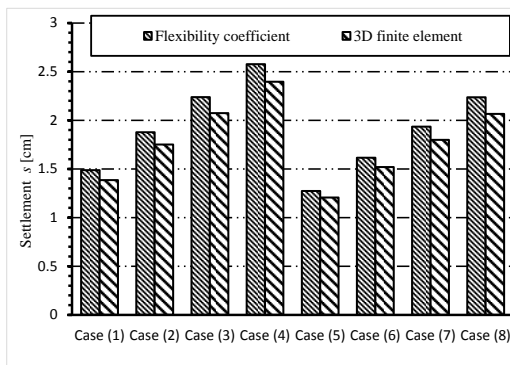


Figure 8: Comparison between settlements, Soil (A)

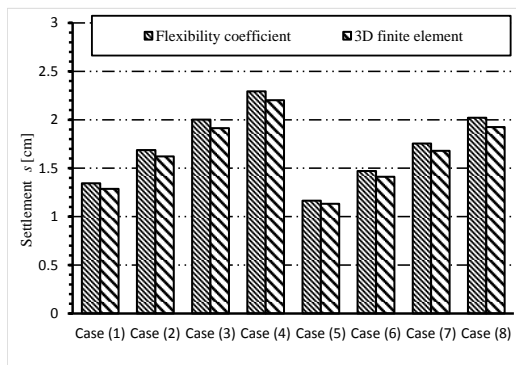


Figure 9: Comparison between settlements, Soil (B)

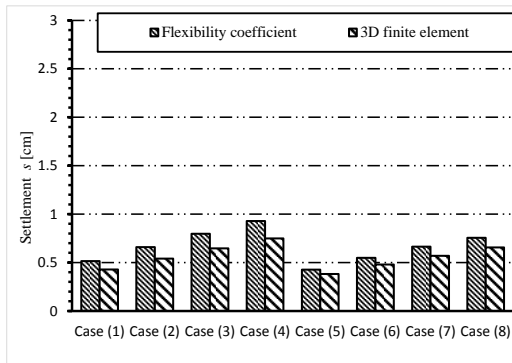


Figure 10: Comparison between settlements, Soil (C)

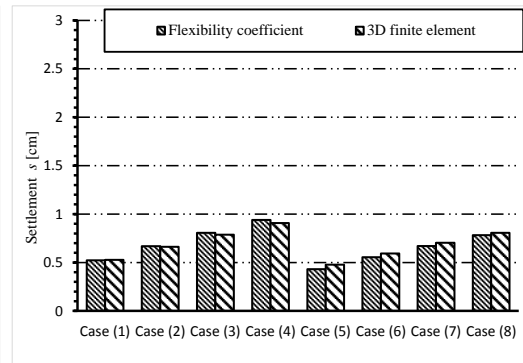


Figure 11: Comparison between settlements, Soil (D)

4.0 Conclusions

An application of *CCT* on barrettes as large-section supports is presented. The proposed technique considers the 3D full interactions between barrette and soil. From application of *CCT* technique on real soil, it can be concluded that:

- Both flexibility coefficient and 3D finite element models can be used safely in the linear analysis of single barrette in cases of half space soil, soil consists of different layers extended from weak to hard layers, and the results are identical.
- For soils that consist of different layers extended from hard layer to weak one, the maximum difference in the settlement between both models is high and reaches twice. It is found that settlements from 3D finite element model are less than those of flexibility coefficient model. This is related to, in 3D finite element mode, the first harder layer is to act as a support for the next weaker soil layer, where the soil is treated as continuum structure connected together and maybe resist soil tension. In this case interface elements between the two layers maybe inserted to enhance the results.
- Flexibility coefficient model can be used safely to model all cases of soil conditions.
- Due to the less number of nodes in flexibility coefficient model rather than 3D finite element model, the first model consumes less computation time in the analysis.

References

- Basu, D., Prezzi, M., Salgado, R., Chakraborty, T. (2008). *Settlement analysis of piles with rectangular cross sections in multi-layered soils*. Computers and geotechnics 35: 563-575.
- Chieruzzi, G., Roy, D., Ayoubian, A. (2013). *Measured and Modeled Settlement of Power Plant on Piled Raft Foundation*. DIF, 37th Annual Deep Foundations Conference, Houston, TX.
- El Gendy, M. (2007). *Formulation of a composed coefficient technique for analyzing large piled raft*. Ain Shams Engineering Journal 42: 29-56.
- El Gendy, M., El Araby, I., Kamal, M. (2013). *Comparative Examination of Single Bored Piles Using International Codes*. Scientific Research Journal of Engineering 5: 796-806.
- El Gendy, M., El Araby, I., Kamal, M. (2014). *Comparative analysis of large diameter bored piles using international codes*. Deep Foundations Institute Journal 8: 15-26.
- El Gendy, M., El Gendy, A. (2017). *Analysis and design of raft and piled Raft-Program ELPLA*. GEOTEC Software Inc., Canada.
- El Labban, A. (2011). *Comparative Studies for Piled Raft Resting on Port Said Clay*. M.Sc. Thesis. Port Said University.
- Fellenius, B., Altaee, A., Kulesza, R., Hayes, J. (1999). *O-Cell testing and FE analysis of 28-m-deep barrette in Manila, Philippines*. Journal of Geotechnical and Environmental Engineering 125: 566-575.
- Hamza, M., Hamed, H. (2000). *Three Dimensional Soil-Structure Analysis of Port-Said East Quay Wall*. Maritime Engineering and Ports II, C.A. Brebbia & J. Olivella, ISBN 1-85312-829-5.
- Hattab, F. (2007). *Vergleichende Untersuchungen numerischer Modelle für die Berechnung von Pfahlplattengründungen*. Diplomarbeit, Matr. NIVERSITÄT SIEGEN.
- Ibrahim, F., El Gendy, M., Salib, R., El Kamash, W. (2009). *Nonlinear analysis of piled raft with 3D-space structure*. Port-Said Engineering Research Journal 13.
- Kamash, W. (2009). *Analysis of Structures on Piled Raft under Earthquake Excitations*. Ain Shams Journal of Civil Engineering 1: 203-2141.
- Kamash, W. (2012). *The positioning and thickness effect for soft clay layer on 3D-building resting on piled raft*. Ain Shams Engineering Journal 3: 17-26.
- Kamash, W., El Gendy, M., Salib, R., Kandil, M. (2014). *Studying of Shear Walls with Piled Raft over Soft Soil against Seismic Loads*. Port Said Engineering Research Journal 18: 144-152.
- Lei, G., Hong, X., Shi, J. (2007). *Approximate three-dimensional analysis of rectangular barrette-soil-cap interaction*. Can. Geotechnical Journal 44: 781-796.
- Lin, S., Lu, F., Kuo, C., Su, T., Mulowayi, E. (2014). *Axial capacity of barrette piles embedded in gravel layer*. Journal of GeoEngineering 9: 103-107.
- Mobarak, W. (2010). *Effect of tie girders on pile caps in Port Said*. M.Sc. Thesis, Faculty of Engineering, Suez Canal University. Port Said.
- Moubarak, A. (2013). *Analysis of Flexible Retaining Walls and Piled Rafts as Settlement Reducer in Port-Said*. PhD thesis, Port Said university.
- Plaxis Bulletin. Issue 32/ autumn 2012. Delft. The Netherlands.
- Rabiei, M. (2009). *Parametric Study for Piled Raft Foundations*. EJGE 14.
- Rabiei, M. (2010). *Effect of Pile Configuration and Load Type on Piled Raft Foundations Performance*. Deep Foundations and Geotechnical Institute Testing (ASCE-GSP 205: 34-41.
- Rabiei, M. (2016). *Piled Raft Design Strategies for High Rise Buildings*. Geotechnical and Geological Engineering 34: 75-85.

- Reda A. (2009). *Optimization of reinforced concrete piled raft*. M.Sc. Thesis, Faculty of Engineering, Suez Canal University. Port Said.
- Russo, G. (1998). *Numerical analysis of piled rafts*. International Journal for Numerical and Analytical Methods in Geomechanics 22: 477-493.
- Seo, H., Basu, D., Prezzi, M., Salgado, R. (2009). *Load-settlement response of rectangular and circular piles in multilayered soil*. Geotechnical and Geoenvironmental Eng: 420-430.
- Shulyatiev, O., Dzagov, A., Bokov, I., Shuliatev S. (2013): *Correction of soil design parameters for the calculation of the foundation based on the result of barrettes static load test*. 18th International Conference on Soil Mechanics and Geotechnical Engineering. Paris: 614-618.
- Thasnanipan, N., Maung, A. and Tanseng, P. (1998). *Barrettes Founded in Bangkok Subsoils, Construction and Performance*. Proceedings of the Thirteenth Southeast Asian Geotechnical Conference: 573-578.
- Thasnanipan, N., Maung, A. and Aye, Z. (2001): *Record load test on a large barrette and its performance in the layered soils of Bangkok*, 5th International conference on deep foundation practice incorporating Piletalk. Singapore: 363-370.